한국공작기계학회 2003 춘계학술대회 논문집 pp.223~228

# Analysis of Shear and Friction chacteristics in End milling with variable cutting condition (Part 1 Up-end milling)

Young Moon Lee*, Seung Han Yang+, Ming Chen++, Seung Il Jang+++

# 절삭조건에 따른 엔드밀링 가공시 전단 및 마찰 특성 분석 (1. 상향 엔드밀링)

이영문*, 양승한+, 첸밍++, 장승일+++

Abstract

In end milling processes, characterized by use of rotating tools, the underformed chip thickness varies periodically with the phase change of tool. In current study, as a new approach to analyze shear behaviors in the shear plane and chip-tool friction behaviors in the chip-tool contact region during an end milling process. In this approach, an up-end milling process is transformed into an equivalent oblique cutting process. Experimental investigations for two sets of cutting tests i.e.. up-end milling and the equivalent oblique cutting tests were performed to verify the presented model.

**Key Words :** Up-end milling, Shear, Friction, Specific cutting energy, Equivalent oblique cutting

## 1. Introduction

End milling is an intermittent cutting process performed by a rotating tool while workpiece is clamped onto a table and feed action is obtained by moving the table. The undeformed-chip thickness and cutting-force components vary periodically with the cutter rotation during the cutting process. Martellotti[1] established the geometric relationships between the tool path and the cutting variables in the intermittent cutting process of milling. Tlusty and Macneil[2] presented a mechanistic model for the prediction of cutting forces by multiplying an undeformed chip area

* 경북대학교 기계공학부 (ymlee@bh.knu.ac.kr)
주소: 702-701 대구시 북구 산격동 1370번지
+ 경북대 기계공학부
++ 중국, 상해교통대 기계공학부
+++ 경북대 대학원 기계공학과

by specific cutting forces in up-end milling, and verified the validity of the model by comparing computed cutting forces with the measured ones .

In a metal cutting process, a chip is produced due to concentrated shear processes that occur at very small intervals in an extremely limited region, referred to as the shear zone. This chip then experiences severe friction with tool rake face before being externally discharged.

Therefore, the study of a cutting process is based on an analysis of the shear process in the shear zone and the friction process in the chip-tool contact region.

Merchant[3] developed an orthogonal cutting analysis that yields a collection of equations enabling the shear and friction processes of two-dimensional continuous cutting to be analyzed.

Shaw et al.[4] analyzed shear and friction processes in oblique cutting and investigated the effects of cutting variables through a series of cutting tests.

Recently, Lee et al.[5] presented a procedure for analyzing shear and chip-tool frictionprocesses using a single point tool. The edge, including a circular nose, is modified to an equivalent straight one, thereby reducing 3-D cutting with a single-point tool to an equivalent oblique cutting. Many researchers[6-8] have added their efforts to a fundamental understanding of intermittent cutting processes but no analysis of the shear and friction processes has yet been attempted.

Accordingly, in the present paper, the shear and friction characteristics of an up-end milling based on an equivalent oblique-cutting model has been analyzed and experimentally verified.

## 2. Up-end milling model

### 2.1 Cutting model

Figure 1 shows a three-dimensional model, including a two-tooth cutter, of an up-end milling process along with the geometrical relations between the tool and workpiece. The maximum undeformed chip thickness, $h_{max}$ is represented by Eq.(1).

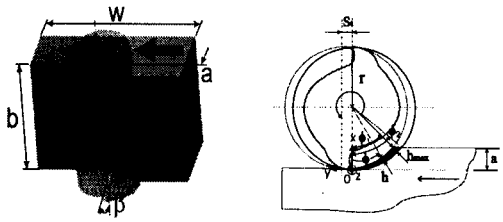


(a) (b)

Fig.1. (a) Schematic and (b) cross section of up-end milling process.

$$h_{\max} = r - \sqrt{(r-a)^2 + [\sqrt{r^2-(r-a)^2} - S_t]^2} \quad (1)$$

In up-end milling, $\phi$ is the tool rotation angle from the base position 0. $\phi_1$ is the rotation angle when $h$ reaches the maximum from the base position 0, and $\phi_2$ is the rotation angle when a cutting edge escapes from the workpiece. $\phi_1$ and $\phi_2$ can be expressed by Eqs.(2) and (3), respectively.

$$\phi_1 = \cos^{-1}\left(\frac{r-a}{r-h_{\max}}\right) \quad (2)$$

$$\phi_2 = \cos^{-1}\left(\frac{r-a}{r}\right) \quad (3)$$

### 2.2 Equivalent oblique cutting model in up-end milling process

To establish an equivalent oblique cutting system equal to an end milling process, the cutting and tool geometrical variables must be matched.

Oblique cutting is the simplest type of three-dimensional cutting processes achieved by a straight cutting edge that is inclined to the coordinate axis perpendicular to cutting velocity vector.

Figure 2 shows a cutting model and unfolded undeformed chips along the workpiece movement direction of up-end milling.

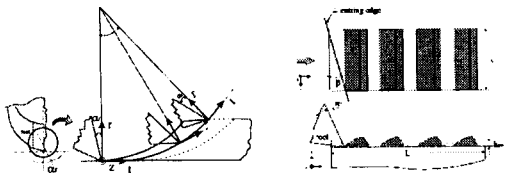

(a) (b)

Fig. 2 (a) Cutting model and (b) spread model of up end-milling process.

In the spread end milling model, the cutting edges meet the z axis with a helix angle($\beta$), which corresponds to the inclination angle($i$) in oblique cutting.

Plus, the radial rake angle $\alpha_r$ in end milling equals the velocity rake angle $\alpha_v$ in oblique cutting. Considering constant intervals are assumed between consecutive cuttings in the spread end milling model, total unfolded length($L$) and average undeformed chip thickness($h_{av}$) can be determined.

The average undeformed chip thickness, $h_{av}$ is determined on the basis of the same volume of chips produced in an end milling and the equivalent oblique cutting process, as in Eq.(4).

$$h_{av} = \frac{a\ S_t\ z}{\pi\ d} \tag{4}$$

Where $d$ is the tool diameter, $z$ is the number of teeth, $S_t$ is the feed per tooth, and $a$ is the radial depth of the cut in the end milling.

The axial depth of cut $b$ and cutting velocity $V$ in an end milling equal the width of cut $b$ and cutting velocity $V$ in equivalent oblique cutting, respectively. Accordingly, the intermittent cutting process can be reduced to an equivalent continuous oblique cutting process with a constant undeformed chip thickness($h_{av}$).

## 2.3 Cutting forces in up-end milling process

Figure 3 shows a cutting force model of up-end milling, where $F_x$, $F_y$, and $F_z$ are the vertical, horizontal, and axial cutting force components, respectively, and $F_r$ and $F_t$ are the radial and tangential cutting force components, respectively.

The cutting forces must be calculated for each tooth as a function of the cutter rotation angle. The total forces are obtained by summing the forces of the teeth engaged in cutting. The relationship between the forces can be expressed as in Eq.(5).

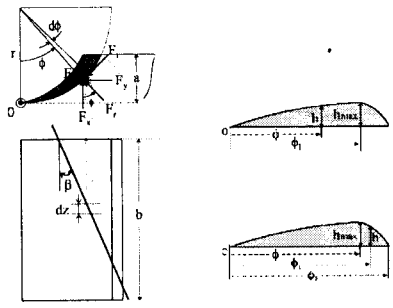

(a) (b)

Fig. 3. (a) Coordinate system for cutting force components and (b) spread undeformed chip cross-sections in up-end milling.

$$\begin{bmatrix} F_x \\ F_y \\ F_z \end{bmatrix} = \begin{bmatrix} \cos\phi & -\sin\phi & 0 \\ \sin\phi & \cos\phi & 0 \\ 0 & 0 & 1 \end{bmatrix} \begin{bmatrix} F_r \\ F_t \\ F_z \end{bmatrix} \tag{5}$$

The infinitesimal radial and tangential cutting forces($dF_r$ and $dF_t$) acting on each tooth are obtained by multiplying the infinitesimal uncut chip area by the specific cutting forces($k_r$ and $k_t$), as in Eqs.(6)and (7).

$$dF_r = k_r dA = k_r h dz \tag{6}$$

$$dF_t = k_t dA = k_t h dz \tag{7}$$

Where $d_z$ is the infinitesimal axial depth of the cut given by Eq.(8).

$$dz = \frac{r}{\tan\beta} d\phi \tag{8}$$

To determine the undeformed chip thickness($h$), the cross section area of the uncut chip, i.e. the shaded area in Fig.3(a), is replaced with an equivalent shaded area with straight base as in

Fig.3(b). When $\phi$ is between the starting point 0 and $\phi_1$, $h$ can be expressed as in Eq.(9).

$$0 < \phi < \phi_1 \qquad h = s_t \cos(90-\phi) = s_t \sin\phi \quad (9)$$

If $\phi$ is between $\phi_1$ and $\phi_2$, $h$ is expressed as in Eq.(10).

$$\phi_1 < \phi < \phi_2 \qquad h = r\left(1 - \frac{\cos\phi_2}{\cos\phi}\right) \quad (10)$$

Figure 4 shows the replaced cross section of the uncut chip including a straight base and 5 intervals where the positions of the cutting edge are distinguished from one another, which is necessary when estimating the cutting forces according to the phase change of tool. The cutting edge is a straight line inclined by $\beta$ and moves from left to right, where, $\phi_3$, $\phi_4$, and $\phi_5$ are as in Eq.(11).

$$\phi_3 = b\tan\beta / r, \quad \phi_4 = \phi_3 + \phi_1, \quad \phi_5 = \phi_3 + \phi_2 \quad (11)$$

When substituting $dz$ and $h$ of Eqs.(8), (9), and (10) in Eqs.(6) and (7), and combining with Eq.(5), the cutting forces for each interval can be obtained as follows.

$[0, \phi_1]$ interval

$$F_x = \int_0^{\phi} (k_r\cos\phi - k_t\sin\phi)\sin\phi\, s_t \frac{r}{\tan\beta}\, d\phi$$

$$F_y = \int_0^{\phi} (k_r\sin\phi + k_t\cos\phi)\sin\phi\, s_t \frac{r}{\tan\beta}\, d\phi \quad (12\text{-}1)$$

$[\phi_1, \phi_2]$ interval

$$F_x = \int_{\phi_1}^{\phi} (k_r\cos\phi - k_t\sin\phi)\, r\, \left(1 - \frac{\cos\phi_2}{\cos\phi}\right)\frac{r}{\tan\beta}\, d\phi + \int_0^{\phi_1} (k_r\cos\phi - k_t\sin\phi)\sin\phi\, s_t \frac{r}{\tan\beta}\, d\phi$$

$$F_y = \int_{\phi_1}^{\phi} (k_r\sin\phi + k_t\cos\phi)\, r\, \left(1 - \frac{\cos\phi_2}{\cos\phi}\right)\frac{r}{\tan\beta}\, d\phi + \int_0^{\phi_1} (k_r\sin\phi + k_t\cos\phi)\sin\phi\, s_t \frac{r}{\tan\beta}\, d\phi \quad (12\text{-}2)$$

$[\phi_2, \phi_3]$ interval

$$F_x = \int_{\phi_1}^{\phi_2} (k_r\cos\phi - k_t\sin\phi)\, r\, \left(1 - \frac{\cos\phi_2}{\cos\phi}\right)\frac{r}{\tan\beta}\, d\phi + \int_0^{\phi_1} (k_r\cos\phi - k_t\sin\phi)\sin\phi\, s_t \frac{r}{\tan\beta}\, d\phi$$

$$F_y = \int_{\phi_1}^{\phi_2} (k_r\sin\phi + k_t\cos\phi)\, r\, \left(1 - \frac{\cos\phi_2}{\cos\phi}\right)\frac{r}{\tan\beta}\, d\phi + \int_0^{\phi_1} (k_r\sin\phi + k_t\cos\phi)\sin\phi\, s_t \frac{r}{\tan\beta}\, d\phi \quad (12\text{-}3)$$

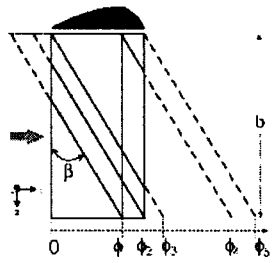


Fig. 4. Cutting edge positions relative to rotation angle of tool in up-end milling.

$[\phi_3, \phi_4]$ interval

$$F_x = \int_{\phi_1}^{\phi_2} (k_r\cos\phi - k_t\sin\phi)\, r\, \left(1 - \frac{\cos\phi_2}{\cos\phi}\right)\frac{r}{\tan\beta}\, d\phi + \int_{\phi-\phi_3}^{\phi_1} (k_r\cos\phi - k_t\sin\phi)\sin\phi\, s_t \frac{r}{\tan\beta}\, d\phi$$

$$F_y = \int_{\phi_1}^{\phi_2} (k_r\sin\phi + k_t\cos\phi)\, r\, \left(1 - \frac{\cos\phi_2}{\cos\phi}\right)\frac{r}{\tan\beta}\, d\phi + \int_{\phi-\phi_3}^{\phi_1} (k_r\sin\phi + k_t\cos\phi)\sin\phi\, s_t \frac{r}{\tan\beta}\, d\phi \quad (12\text{-}4)$$

$[\phi_4, \phi_5]$ interval

$$F_x = \int_{\phi-\phi_3}^{\phi_2} (k_r\cos\phi - k_t\sin\phi)\, r\, \left(1 - \frac{\cos\phi_2}{\cos\phi}\right)\frac{r}{\tan\beta}\, d\phi$$

$$F_y = \int_{\phi-\phi_3}^{\phi_2} (k_r\sin\phi + k_t\cos\phi)\, r\, \left(1 - \frac{\cos\phi_2}{\cos\phi}\right)\frac{r}{\tan\beta}\, d\phi \quad (12\text{-}5)$$

## 3. Cutting experiments

Two sets of experiments tests i.e., up-end milling and equivalent oblique cutting tests were performed to verify the validity of proposed force model under various cutting conditions.

End-mills of 8mm diameter with 20° helix angles were used in the end milling tests.

The cutting tool in equivalent oblique cutting was a TT1500 insert with a chip former designated as 20° inclination angle.

Table 1 shows the cutting test conditions of up-end milling and equivalent oblique cutting. The three cutting force components were measured using a piezo-type tool dynamometer and the force signals were digitized and stored using a micro-processor-controlled data acquisition system.

Table 1 Cutting conditions

| Up-end milling | |
|---|---|
| Work material | SM45C |
| Radial depth of cut, $a$ (mm) | 3 |
| Axial depth of cut, $b$ (mm) | 2 |
| Cutting velocity, $V$ (m/min) | 10.2, 15.9, 22.5 |
| Radial rake angle, $\alpha_r$ (deg.) | 6 |
| Helix angle, $\beta$(deg.) | 20 |
| Number of teeth, $Z$ | 2 |
| Feed per tooth, $S_t$ (mm) 0.2051,0.2302,0.2428,0.2554,0.2805 | |
| Equivalent Oblique cutting | |
| Work material | SM45C |
| Width of cut, $b$ (mm) | 2 |
| Cutting velocity, $V$ (m/min) | 10.2, 15.9, 22.5 |
| Velocity rake angle, $\alpha_v$ (deg.) | 6 |
| Inclination angle, $i$ (deg.) | 20 |
| Undeformed chip thickness, $h_{av}$ (mm) 0.049,0.055,0.058,0.061,0.067 | |

## 4. Results and discussions

### 4.1 Cutting forces

Substituting the measured cutting force components, $F_x$ and $F_y$ for Eq.(12), the specific cutting forces, $k_r$ and $k_t$ can be obtained. The tangential($F_t$) and radial($F_r$) cutting forces are estimated by multiplying the undeformed cut area by the specific cutting forces. In the equivalent oblique cutting model, the main($F_y$), the feed($F_z$), and the thrust($F_x$) cutting forces correspond to the tangential($F_t$), the radial($F_r$), and the axial($F_z$) cutting forces of the end milling model, respectively. Fig. 5 shows the measured forces($F_x$, $F_y$), and tangential and radial forces($F_r$, $F_t$), with the lowest (0.2051mm/tooth) and largest (0.2805mm /tooth) feed per tooth and the lowest(10.2m/min) and largest(22.5m/min) cutting velocity based on the given conditions. Figure 6 shows the averaged end milling forces and measured forces of the equivalent oblique cutting versus the equivalent underformed chip thickness and cutting velocity.

There was no significant difference between the two sets of cutting forces. Therefore, as a first approximation, the appropriateness of analyzing the friction and shear processes of an intermittent cutting using the equivalent oblique cutting system was confirmed.

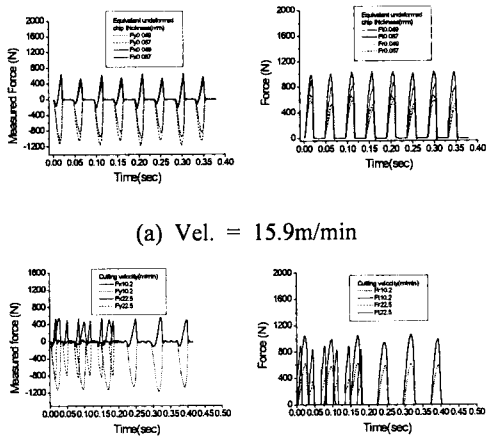


(a) Vel. = 15.9m/min

(b) $S_t$ = 0.2302mm/tooth

Fig. 5. Measured forces and tangential and radial forces($F_r$ and $F_t$) in up-end milling.

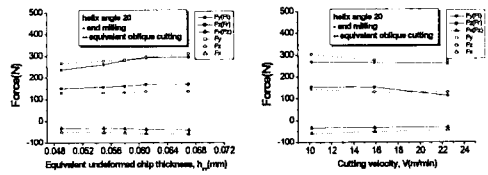


(a) Vel. = 15.9m/min (b) $S_t$ = 0.2302mm/tooth

Fig. 6. Average cutting forces in up-end milling and equivalent oblique cutting.

### 4.2. Shear and friction characteristics

Table 2 shows the shear and friction characteristic factors in the up-end milling and the equivalent oblique cutting under the given cutting conditions presented in Table 1. The factors were calculated by substituting the replaced cutting forces into the oblique cutting model[5]. The friction forces and specific friction energies consumed in the end

milling process were somewhat larger than those consumed in the equivalent oblique cutting.

While the shear forces and specific shear energies were vice versa. In case of vel.=15.9m/min, 66 ~ 68% and 70 ~ 71% of the total energy was consumed in the shear processes in the end milling and the equivalent oblique cutting, respectively.

In case of $S_t$=0.2302mm/tooth, 70 ~ 72% and 75 ~ 72% of the total energy was consumed in the shear processes in the end milling and the equivalent oblique cutting, respectively.

In addition, the specific cutting energy decreased with an increase in the undeformed thickness and cutting velocity in the end milling process. As such, these results coincided well with those of previous studies[4),(5)].

Table 2 Shear and friction characteristics

(a) Vel. = 15.9m/min

| | Up-end milling | Equivalent oblique cutting |
|---|---|---|
| | 20° | 20° |
| **Friction Characterics** | | |
| Friction force, $F_f$ (N) | 175.2 ~ 199.5 | 161.8 ~ 173.8 |
| Specific friction energy, $u_f$(MPa) | 812.7 ~ 717.8 | 783.3 ~ 682.1 |
| **Shear Characteristics** | | |
| Shear force, $F_s$ (N) | 150.3 ~ 197.1 | 189.9 ~ 230.8 |
| Specific shear energy, $u_s$(MPa) | 1600.6 ~ 1548.5 | 1957.7 ~ 1736.8 |
| **Cutting Characteristics** | | |
| Specific cutting energy, $u$(MPa) | 2413.3 ~ 2266.3 | 2711.8 ~ 2315.1 |
| $u_f/u$ | 0.34 ~ 0.32 | 0.29 ~ 0.30 |
| $u_s/u$ | 0.66 ~ 0.68 | 0.71 ~ 0.70 |

(b) $S_t$ = 0.2302mm/tooth

| | Up-end milling | Equivalent oblique cutting |
|---|---|---|
| | 20° | 20° |
| **Friction Characterics** | | |
| Friction force, $F_f$ (N) | 188.7 ~ 149.4 | 179.6 ~ 163.4 |
| Specific friction energy, $u_f$(MPa) | 736.6 ~ 654.1 | 683.5 ~ 691.9 |
| **Shear Characteristics** | | |
| Shear force, $F_s$ (N) | 187.8 ~ 186.9 | 227.9 ~ 196.5 |
| Specific shear energy, $u_s$(MPa) | 1701.8 ~ 1711.2 | 2076.6 ~ 1803.9 |
| **Cutting Characteristics** | | |
| Specific cutting energy, $u$(MPa) | 2438.4 ~ 2365.3 | 2760.1 ~ 2495.8 |
| $u_f/u$ | 0.30 ~ 0.28 | 0.25 ~ 0.28 |
| $u_s/u$ | 0.70 ~ 0.72 | 0.75 ~ 0.72 |

## 5. Conclusions

The equivalent oblique cutting model has been proposed to analyze the friction and shear processes of an up-end milling process which has not been attempted previously. The model was verified through two sets of experiments.

The experimental results show that the proposed model is suitable to analyze the shear and chip-tool frictional characteristics of up-end milling process.

## REFERENCES


1. Martellotti, M.E., 1941, "An Analysis of the Milling Process," Trans. ASME, Vol. 63, pp. 677-700.

2. Tlusty, J. and Macneil, P., 1975, "Dynamics of Cutting Forces in End Milling," Annals of CIRP, Vol. 24, pp. 21-25.

3. Merchant, M.E., 1945, "Mechanics of the metal cutting process, I. Orthogonal cutting and a type 2 chip", J. Appl. Phys., Vol. 16 No. 5, pp. 267-275.

4. Shaw, M. C., Cook, N. H., and Smith, P. A., 1951, "The Mechanics of Three dimensional Cutting Operations," Trans. ASME, Vol. 73, pp. 1055-1064.

5. Lee, Y. M., Choi, W. S., and Song, T. S., 2000, "Analysis of 3-D Cutting Process with Single Point Tool", J. KSPE, Vol.1 No.1, pp.15-21.

6. Wang, J. J. and Liang, S. Y., 1996, "Chip Load Kinematics in Milling with Radial Cutter Runout," ASME, J. Eng. for Ind., Vol. 118, pp. 111-116,

7. Yang, M. Y. and Choi, J. G., 1998, "A Tool Deflection Compensation System for End Milling Accuracy Improvement", ASME, J. Man. Sci. and Eng., Vol. 120, pp. 222-229.

8. Lazoglu, I. and Liang, S. Y., "Modeling of Ball-End Milling Forces with Cutter Axis Inclination," ASME, J. Man. Sci. and Eng., Vol. 122, pp. 3-11, 2000.